Influence of Ferroelectric Polarization on the Equilibrium Stoichiometry of Lithium Niobate (0001) Surfaces

Sergey V. Levchenko and Andrew M. Rappe*

The Makineni Theoretical Laboratories, Department of Chemistry, University of Pennsylvania, Philadelphia, Pennsylvania 19104-6323, USA

(Received 2 July 2007; published 23 June 2008)

We present a first-principles density functional theory study predicting the relative thermodynamic stability of ferroelectric lithium niobate ($LiNbO_3$) (0001) surfaces of different stoichiometry. We predict that the equilibrium stoichiometries are different for the positively and negatively polarized $LiNbO_3$ surfaces under the same conditions. Based on the modern theory of polarization, we demonstrate how a simple ionic model can be used to calculate surface charges for ferroelectric surfaces with intrinsic polar stacking. It is found that surface charge passivation by ions is thermodynamically favored over passivation by mobile carriers in a wide range of chemical potentials.

DOI: 10.1103/PhysRevLett.100.256101 PACS numbers: 82.65.+r, 68.35.−p, 68.35.Md, 77.84.Dy

Knowledge of stabilization mechanisms of polar oxide surfaces is important for understanding their functional properties in both natural and technological processes [1,2]. In the absence of electrodes, charged surfaces tend to lower their energy by surface metallization, by reconstruction, by molecular adsorption, or by varying surface stoichiometry [3–9]. A particular stabilization mechanism determines stoichiometry and oxidation state of atoms at the surface and, consequently, greatly affects surface chemical properties. For example, a change in surface stoichiometry alters preferred adsorption sites, energetics, and atom exchange between the surface and the reactants and products in surface chemical reactions.

From this point of view, surfaces of ferroelectric (FE) oxide materials are an interesting subset of polar surfaces. The polarity of ferroelectric surfaces can be tuned or even reversed by a well-controlled external perturbation, such as the electric field and temperature. In addition to providing a novel probe to study the stabilization mechanisms, this property brings up new possibilities for optimization of material functionality, as well as dynamical control of heterogeneous catalysts [10].

The surface structure and stoichiometry are determined not only by the atomic composition and structure of the bulk material but also by the composition, temperature, and pressure of the gaseous environment in contact with the surface. The effect of the environment on FE surfaces is especially difficult to predict, because of the subtle balance between the ionic and covalent character of the metal-oxygen bonds. For example, the magnitude and even the direction of polarization in FE thin films can be changed by gaseous conditions [11].

In this Letter, we present a theoretical study of FE $LiNbO_3$ (LN) (0001) surfaces, which is of both fundamental and practical interest. Although LN is a complex bimetallic oxide, it has a single stable crystal phase, with ferroelectric polarization directed along (0001), that is also an intrinsically polar direction. Because of these properties, LN has been attracting attention as a heterogeneous catalyst for a long time [12–15] and is being actively studied at the moment [16,17].

Only a few experimental studies of the (0001) LN surface structure have been reported [12,18–20], mostly for an unpoled crystal. Mass-spectrometric investigations of species evaporated from positive and negative surfaces of a single-domain LN crystal upon annealing at $T \geq 1200$ K revealed a substantially greater evaporation rate for LiO, Li, and O_2 from the positive surface, with the evaporation of Li and O_2 being almost absent and evaporation of LiO being an order of magnitude smaller for the negative surface [20].

We calculate the relative thermodynamic stability of positive and negative polarization LN surfaces of different stoichiometry. We predict changes in the equilibrium surface stoichiometry under a range of temperatures and oxygen pressures. We find that the stoichiometry of positive and negative surfaces under the same experimental conditions should be quite different.

Details of DFT calculations.—Density functional theory (DFT) total energies of LN, Li_2O, Nb_2O_5, and bulk Li and Nb have been obtained using the norm-conserving nonlocal pseudopotential plane wave method and the generalized gradient approximation (GGA) of the exchange-correlation functional [21], as implemented in the ABINIT package [22] and in our in-house code BH.

For the FE LN (0001) surface calculations, we use a slab consisting of seven -Li-O_3-Nb- trilayers plus Li_u-O_v-Nb- as a positive surface termination and -Li_x-O_y as a negative surface termination, $u = 0, 1, 2$, $x = 0, 1$, $v = 1, 2, 3, 4$, and $y = 0, 1, 2, 3$ (all possible combinations for each surface have been analyzed). Based on the results, we concluded that the chosen maximum content of Li and O atoms at the surfaces is sufficient. Only the 1×1 surface unit cell is considered. Although we expect that considering larger surface unit cells is required to pinpoint the exact stoichiometry of real surfaces, we believe that the trends

and physical picture derived from our results will not be altered by this limitation. The in-plane lattice parameters, as well as the atomic positions of the middle three trilayers, have been fixed at bulk values. The outer two trilayers on each face and all of the terminating atoms in the slab unit cell are allowed to relax in all directions, and the threefold rotation symmetry has been slightly broken to make sure that the symmetric geometry is not a saddle point. A vacuum region of ≈ 17 Å separates one slab from its supercell images. The dipole correction [23] is used to remove the effect of the artificial electric field created by the slab images on both electronic structure and equilibrium geometry.

Surface free energy.—We follow the *ab initio* thermodynamics approach described in previous work [24–27]. The two slab surfaces cannot be made equivalent because of the FE symmetry breaking, so that the surface free energy cannot be calculated separately for each surface. However, since we are interested in *relative* surface energies, the free energies for different terminations can be instructively compared if the other surface is kept the same.

DFT calculations correspond to $T = 0$ and constant volume, not pressure. Therefore, in addition to the DFT total energy, one must also consider the entropy and pV terms [26]. Following [26], we estimate the upper limit for the total contribution of these terms to be 0.2–0.3 eV/unit cell (see [28] for information on the bulk LN fundamental vibrations). Since this uncertainty does not change any conclusions of this work, we approximate the Gibbs free energy by the DFT total energy.

The range of possible chemical potentials μ_i, $i =$ Li, Nb, O, is constrained by the stability of various phases. First, we focus on chemical potential values for which the bulk LN phase is stable. This allows us to express one of μ_i through the other two. We choose to express μ_{Nb} in terms of μ_{O} and μ_{Li}, because they are more easily controlled in experiments. We also exclude values of chemical potentials at which other condensed phases such as solid Li, Nb, Li_2O, and Nb_2O_5 or liquid O_2 start to precipitate [26].

It is convenient to choose the free energies of each elemental phase at standard conditions ($T = 298.15$ K and $p = 1$ atm) as zero for the corresponding chemical potential. With this convention, all bulk and slab oxide energies are free energies of formation.

It is known [29] that the GGA functional overestimates binding in molecules. In fact, our DFT-GGA O_2 binding energy is 0.6 eV/atom higher than the experimental value. To correct for this error, we use the experimental value in calculations.

Results and discussion.—FE LN can be viewed as -Li-O_3-Nb- trilayers stacked along (0001) [30]. Paraelectric (PE) LN has -LiO_3-Nb- bilayers; the FE instability involves Nb displacements from the centers of oxygen octahedra, and Li movement out of oxygen planes, along the (0001) direction. Figure 1 shows the -Li-O_3-Nb- trilayers and the landscape of the unrelaxed cleavage surface.

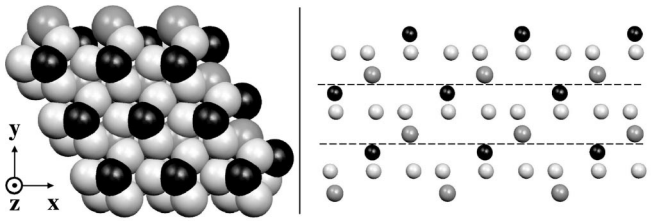

FIG. 1. Bulklike LN (0001) surface (left) and -Li-O_3-Nb- trilayers (right) with the normal along the z axis. Li is black, Nb is gray, and O is light gray.

The most stable LN surface terminations under different ambient conditions in the absence of foreign adsorbates are shown in Fig. 2. Space-fill models of some of the stable surface terminations are presented in Fig. 3.

The theoretical (DFT total energy differences) and experimental (at standard conditions) formation energies for different phases are summarized in Table I. For LN, energy is reported per $LiNbO_3$ unit. Since Nb_2O_5 has different crystal types depending on heat treatment, and each type has a complicated crystal structure with long-range ordering, we decided to use the experimental Nb_2O_5 energy of formation in our calculations.

The values of Li and O chemical potentials at which only the bulk LN phase is stable fall within the trapezoid. Since the surfaces can equilibrate much faster than the bulk, we do not confine μ_{O} and μ_{Li} to the trapezoid.

When the spontaneous polarization vector is directed away from the surface (negative surface), the -Li-O termination is favored under most conditions (Fig. 2, left). The positive surface contains, in general, more oxygen than the negative surface at similar conditions (Fig. 2, right). Under chemical potential conditions where bulk LN is stable, the Li_2-O_3-Nb- termination (i.e., one extra Li atom per surface cell above stoichiometric trilayers) has the lowest free energy for all conditions. An interesting feature of the

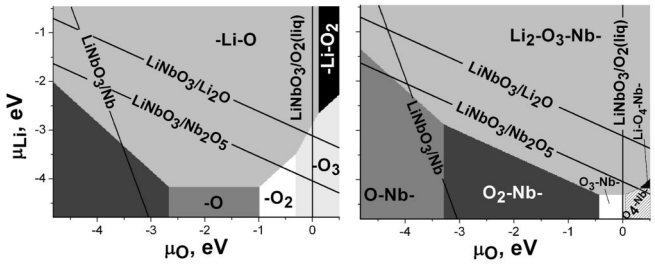

FIG. 2. Stable surface terminations of negative (left) and positive (right) surfaces of LN. The terminations are labeled with hyphens. The unlabeled region corresponds to an Nb-terminated surface. The black lines denote boundaries beyond which new bulk phases (shown on corresponding lines) start to precipitate on the LN surfaces. The region where only the bulk LN phase is stable is within the trapezoid formed by the black lines.

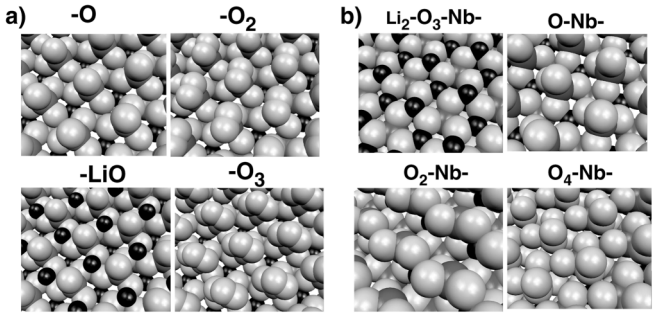

FIG. 3. Space-fill models of LN (a) negative and (b) positive surface terminations stable at various conditions. Li is black, Nb is gray, and O is light gray.

Li_2-O_3-Nb- termination is that one Li relaxes down into the top oxygen plane, while the other Li stays above the oxygen plane. Our calculations suggest that the surface loses 2(LiO) and becomes terminated by O-Nb- under low μ_O conditions. It is interesting to note that the positive surface prefers to lose two Li atoms at low μ_{Li} instead of losing them one by one. Note that we did not consider Li coverages other than 0, 1, or 2 Li atoms per unit cell. It is possible that an intermediate Li coverage could be stable for low μ_{Li}. Nevertheless, our calculations clearly show the propensity of the positive surface to be enriched with Li relative to the negative surface.

The phase diagrams do not change qualitatively if we do not correct for the difference between experimental and calculated bond energy in O_2. The use of the calculated bond energy results in stabilizing oxygen-poor surfaces but no new terminations enter the diagrams.

The stability of the preferred terminations of positive and negative surfaces of LN can be explained by passivation of surface charges with ions, provided that the surface charges are calculated correctly.

First, we develop an ionic model based on formal oxidation states, $q_{Nb} = +5e$, $q_O = -2e$, $q_{Li} = +e$, to calculate the surface charges of the stoichiometric PE-like LN slab with equally spaced LiO_3 and Nb layers, terminated with a LiO_3 layer on one side and a Nb layer on the other side. With this model, the stoichiometric PE-like slab would have surface charges of $-5e/2$ per surface unit cell on the LiO_3- termination and $+5e/2$ on the -Nb termination. The potential difference created by these charges is $\Delta\phi \approx 20$ V/Å. Therefore, these charges must be passivated by mobile charges (electron transfer), stoichiometry changes (adding charged ions), or any combination.

Let us imagine for a moment that the surfaces are created instantly, so that the ionic charges remain the same as in the bulk. Since $\Delta\phi$ is much greater than the potential required to transfer electrons across the band gap (3.7 eV for LN), the surface charges will be almost completely passivated by the electron transfer. However, as explained below, our results demonstrate that passivation by ions is thermodynamically favored over the passivation by the mobile charges.

TABLE I. Theoretical and experimental enthalpies of formation (eV) for the relevant phases.

	Theory	Exp.
$LiNbO_3$	−14.1	−13.872 ± 0.030 [31]
Li_2O	−6.2	−6.23 [32]
Nb_2O_5		−19.755 [32]
O	3.2	2.58 [32]

Among stoichiometric PE-like phases (holding all layers fixed with O and Li coplanar), we find that transfers of O (ionic charge of $-2e$) or O_2Li ($-3e$) from the LiO_3 surface to the Nb surface are the most stable, lowering the energy by 4.6 eV/cell (converged with respect to the slab thickness). Within a 1×1 surface cell, these two choices optimally reduce the model surface charges, from $\mp 5e/2$ per surface cell to $\mp e/2$ with O transfer or to $\pm e/2$ with O_2Li transfer. So, the PE case illustrates the idea that, when possible, passivation with ions is more favorable than passivation with mobile charges.

Extending this model to FE LN, we note that the polarization P_{PE} of the PE LN is nonzero, because of the polar stacking of ionic layers composed of ions whose net charge per unit cell is odd. With $P_{PE} \neq 0$, the meaningful FE polarization is $P_{FE} - P_{PE}$, computed with the same layer stacking within the unit cell for FE and PE. We use the Berry's phase approach [33] to compute polarization of bulk LN. This approach allows us to calculate polarization of a nonmagnetic insulator within an even integer multiple $2N$ of a polarization quantum. In the case of LN, the polarization quantum per hexagonal unit cell is $eR/\Omega = e/S$, where R is the length of the lattice vector along the (0001) direction, Ω is the volume of the unit cell, and S is the area of the surface unit cell. We find $P_{FE} - P_{PE} = (2N \times 0.69 + 0.86)$ C/m^2 $\approx (2N + 5/4)e/S$. By analyzing the polarization change as Born effective charges times atomic displacements, we find that the polarization change going from PE to FE is correct for $N = 0$. Thus, the FE phase transition adds a surface charge of $5e/4$ per surface cell to the stoichiometric Li-O_3 (0001) surface and $-5e/4$ to the Nb-terminated surface, leaving the Li-O_3- termination with a net bound surface charge of $-5e/4$ and the -Nb termination with $+5e/4$ in the FE phase.

The above polarization and surface charge analysis explains the observed stable surface stoichiometries of the FE LN surfaces. The stoichiometric Li-O_3-Nb- (0001) surface has a net bound charge of $-5e/4$. The addition of an extra Li atom (surface denoted Li_2-O_3-Nb-) stabilizes a hole and, within the simple ionic model, reduces the charge to $-e/4$ in the insulating state. On the bottom surface, the Nb termination has a bound charge of $+5e/4$, and addition of -O-Li stabilizes the charge of $-e$ reducing the net

surface charge to $+e/4$. Depending on conditions and history, this last $\pm e/4$ can be passivated with mobile charges or with submonolayer coverage of additional ions. Thus, our first-principles thermodynamics findings demonstrate the preference for passivation of the surface charge with ions in this system. The surface charge can be calculated from the simple ionic model by taking into account both ferroelectric polarization and intrinsic polar stacking.

Our calculations explain the observed differences in evaporation rates of LiO, Li, and O_2 from positive and negative surfaces of a single-domain LN crystal at elevated temperatures [20]. In the experiment, the evaporation of Li and O_2 from the negative surface was negligibly slow, while the evaporation of LiO was an order of magnitude slower than the evaporation of the same species from the positive surface. According to our calculations, the positive surface contains more oxygen and lithium than the negative one, and it loses oxygen and lithium (Li_2-O_3-Nb- → O-Nb-) at higher chemical potentials and, consequently, lower temperature than the negative surface (-Li-O → Nb-terminated).

Conclusions.—For the first time, we present an extension of first-principles thermodynamics to a three-component FE surface with intrinsic polar stacking. Our calculations predict substantial differences in stoichiometry of thermodynamically stable positive and negative (0001) surfaces of FE LN. The surface charges can be calculated from Berry's phase analysis of bulk polarization and simple ionic modeling. The potential created by the surface charges is much greater than the band gap and is screened almost completely by the mobile carriers. However, the analysis of thermodynamic stability reveals that passivation with ions is favored over the passivation with electrons and holes.

The stable surface terminations are those providing low-energy surface states to accommodate electron and hole screening the surface charges. The positive surface (to which polarization is directed) contains more oxygen than the negative surface, to passivate the surface charge induced by the ferroelectric transition. It also contains more lithium, because Li atoms provide low-energy surface states to accommodate the screening hole. Because of the increased content of oxygen and lithium, the evaporation from the positive surface occurs more readily than from the negative one.

This work was supported by the Office of Naval Research under Grant No. N00014-00-1-0372 and by the Department of Energy, Office of Basic Energy Sciences, under Grant No. DE-FG02-07ER15920. Computational support was provided by a Challenge grant from the HPCMO of the U.S. Department of Defense.

*rappe@sas.upenn.edu; http://www.sas.upenn.edu/rappegroup

[1] W. H. Casey and C. Ludwig, Nature (London) **381**, 506 (1996).
[2] J. Jupille, Surf. Rev. Lett. **8**, 69 (2001).
[3] C. Noguera, J. Phys. Condens. Matter **12**, R367 (2000).
[4] F. Finocchi, A. Barbier, J. Jupille, and C. Noguera, Phys. Rev. Lett. **92**, 136101 (2004).
[5] A. Subramanian, L. D. Marks, O. Warschkow, and D. E. Ellis, Phys. Rev. Lett. **92**, 026101 (2004).
[6] V. Staemmler, K. Fink, B. Meyer, D. Marx, M. Kunat, S. G. Girol, U. Burghaus, and Ch. Wöll, Phys. Rev. Lett. **90**, 106102 (2003).
[7] O. Dulub, U. Diebold, and G. Kresse, Phys. Rev. Lett. **90**, 016102 (2003).
[8] C. Ruberto, Y. Yourdshahyan, and B. I. Lundqvist, Phys. Rev. Lett. **88**, 226101 (2002).
[9] B. Meyer, Phys. Rev. B **69**, 045416 (2004).
[10] A. M. Kolpak, I. Grinberg, and A. M. Rappe, Phys. Rev. Lett. **98**, 166101 (2007).
[11] D. D. Fong *et al.*, Phys. Rev. Lett. **96**, 127601 (2006).
[12] T. Choso, M. Kamada, and K. Tabata, Appl. Surf. Sci. **121/122**, 387 (1997).
[13] K. Tabata, M. Kamada, T. Choso, and Y. Nagasawa, J. Chem. Soc., Faraday Trans. **94**, 2213 (1998).
[14] K. Tabata, M. Kamada, T. Choso, and H. Munakata, Appl. Surf. Sci. **125**, 93 (1998).
[15] Z. Li, T. Yu, and Z. Zou, Appl. Phys. Lett. **88**, 071917 (2006).
[16] Y. Yun and E. I. Altman, J. Am. Chem. Soc. **129**, 15 684 (2007).
[17] J. Garra and J. Vohs (private communication).
[18] K. Tabata, T. Choso, and Y. Nagasawa, Surf. Sci. **408**, 137 (1998).
[19] K. Tabata, M. Kamada, T. Choso, and H. Munakata, J. Phys. Chem. B **101**, 9161 (1997).
[20] A. Y. Lushkin, V. B. Nazarenko, K. N. Pilipchak, V. F. Shnyukov, and A. G. Naumovets, J. Phys. D **32**, 22 (1999).
[21] J. P. Perdew, K. Burke, and M. Ernzerhof, Phys. Rev. Lett. **77**, 3865 (1996).
[22] X. Gonze *et al.*, Comput. Mater. Sci. **25**, 478 (2002).
[23] L. Bengtsson, Phys. Rev. B **59**, 12 301 (1999).
[24] X. G. Wang *et al.*, Phys. Rev. Lett. **81**, 1038 (1998).
[25] X. G. Wang, A. Chaka, and M. Scheffler, Phys. Rev. Lett. **84**, 3650 (2000).
[26] K. Reuter and M. Scheffler, Phys. Rev. B **65**, 035406 (2001).
[27] S. J. Jenkins, Phys. Rev. B **70**, 245401 (2004).
[28] H. R. Xia *et al.*, J. Appl. Phys. **98**, 033513 (2005).
[29] F. Furche, Phys. Rev. B **64**, 195120 (2001).
[30] R. S. Weis and T. K. Gaylord, Appl. Phys. A **37**, 191 (1985).
[31] I. Pozdnyakova, A. Navrotsky, L. Shilkina, and L. Reznitchenko, J. Am. Ceram. Soc. **85**, 379 (2002).
[32] M. W. Chase, Jr., J. Phys. Chem. Ref. Data **9**, 1 (1998).
[33] D. Vanderbilt and R. D. King-Smith, Phys. Rev. B **48**, 4442 (1993).